

Supporting Information

Phosphonated mesoporous silica nanoparticles bearing ruthenium complexes used as
molecular probe for tracking oxygen levels in cells and tissues

Yui Umehara,¹ Yu Kimura,¹ Freddy Kleitz,² Tatsuya Nishihara,³ Teruyuki Kondo*¹ and

Kazuhito Tanabe*³

¹Department of Energy and Hydrocarbon Chemistry, Graduate School of Engineering,
Kyoto University, Nishikyo-ku, Kyoto, 615-8510, Japan

²Department of Inorganic Chemistry – Functional Materials, Faculty of Chemistry,
University of Vienna, Währinger Straße 42, A-1090, Vienna, Austria

³Department of Chemistry and Biological Science, College of Science and Engineering,
Aoyama Gakuin University, 5-10-1 Fuchinobe, Chuo-ku, Sagamihara, 252-5258, Japan

*Corresponding author

Dr. Teruyuki Kondo
Phone: +81-75-383-7055 FAX: +81-75-383-2504
e-mail: teruyuki@scl.kyoto-u.ac.jp

Dr. Kazuhito Tanabe
Phone: +81-42-759-6229 FAX: +81-42-759-6493
e-mail: tanabe.kazuhito@chem.aoyama.ac.jp

Table S1. Weight Loss of Particles in Each Step in Scheme 1.^a

	pM-Ru-48-100	pM-Ru-41-100	pM-Ru-48-50
Particle I	45%	43%	29%
Particle II	40%	35%	28%
Particle III	11%	5.2%	8.8%
Particle IV	16%	15%	18%

^aWeight loss was estimated by using thermogravimetric analysis.

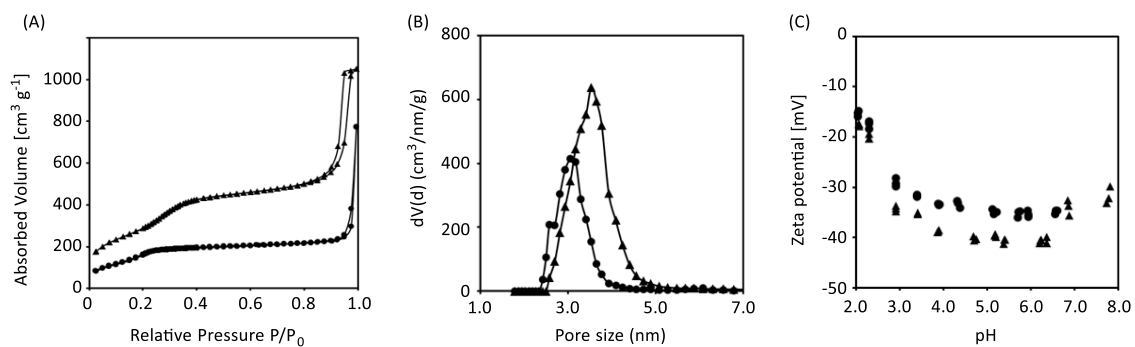


Figure S1. (A) N₂ physisorption isotherms of pM-Ru-41-100 (triangle) and pM-Ru-48-50 (circle). The analysis was conducted at -196 °C. (B) Pore size distribution analysis of pM-Ru-41-100 (triangle) and pM-Ru-48-50 (circle). (C) The effect of pH on zeta potentials of pM-Ru-41-100 (triangle) and pM-Ru-48-50 (circle).

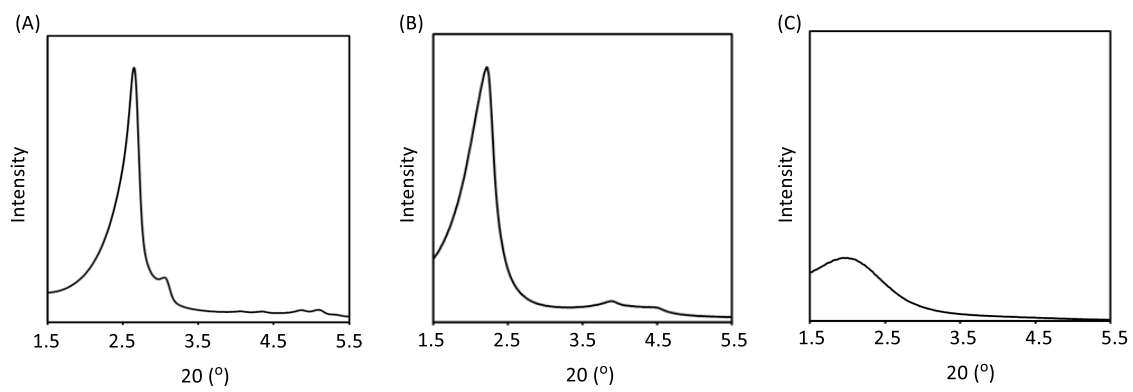


Figure S2. XRD patterns of pM-Ru-48-100 (A), pM-Ru-41-100 (B) and pM-Ru-48-50 (C).



Figure S3. Nanoparticles dispersed in aqueous solution containing sodium phosphate buffer (5 mM, pH 7.0). Left: Nanoparticles with phosphonate groups on their external surface (pM-Ru). Right: Nanoparticles without phosphonate groups on their external surface (M-Ru).

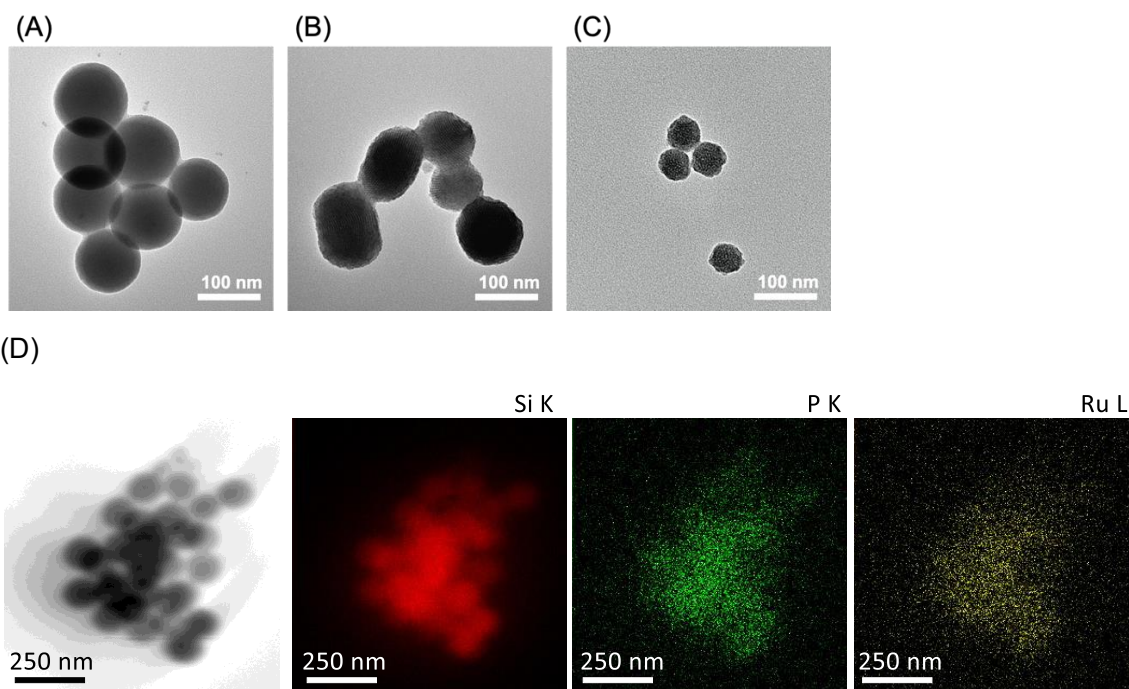


Figure S4. TEM images of (A) pM-Ru-48-100, (B) pM-Ru-41-100 and (C) pM-Ru-48-50. (D) EDX images of pM-Ru-48-100.

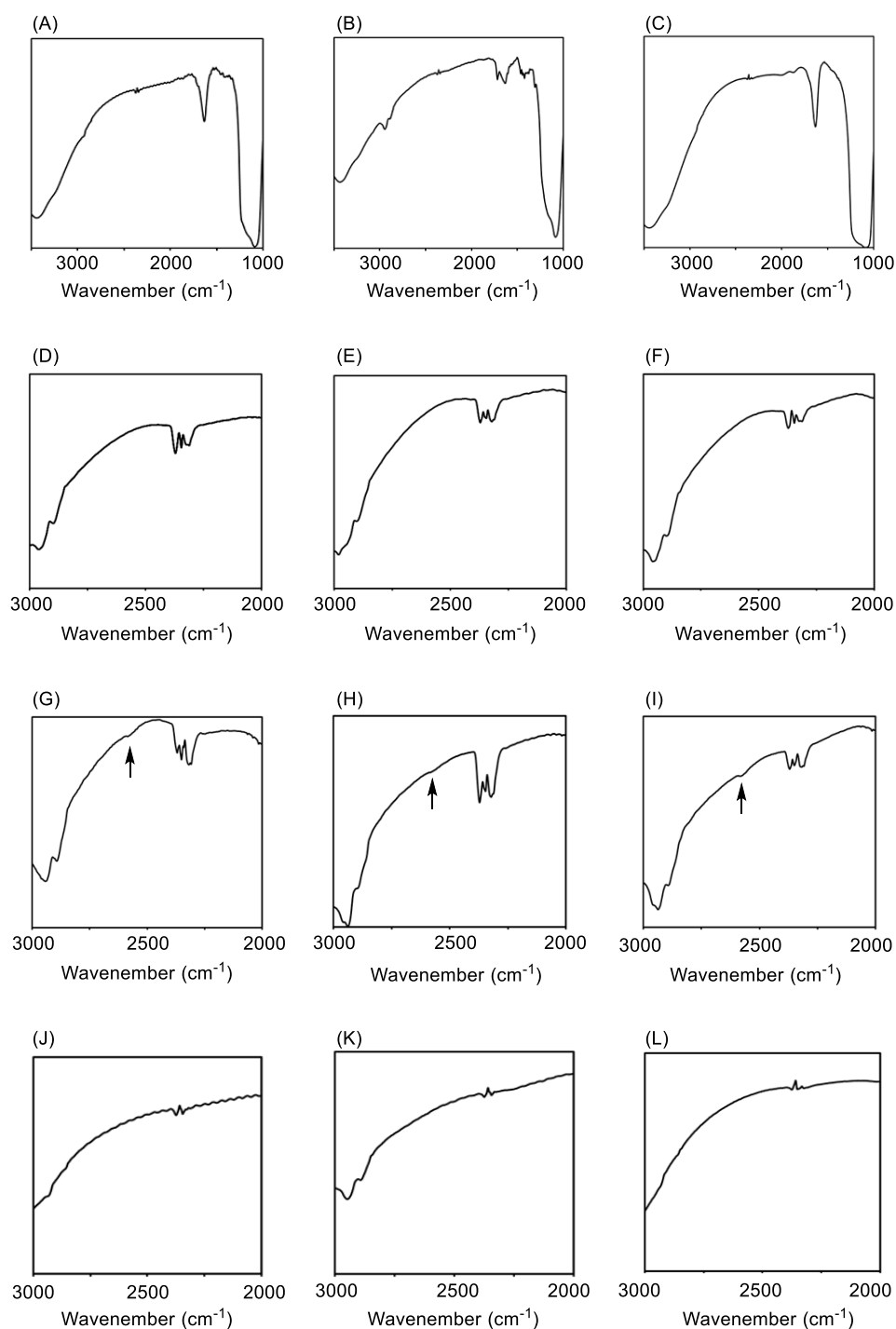


Figure S5. IR spectra of pM-Ru-48-100 (A, D, G, J), pM-Ru-41-100 (B, E, H, K) and pM-Ru-48-50 (C, F, I, L). (A-C) IR spectra (1000-3500 cm^{-1}) of Particle IV. (D-F) Enlarged view of the spectra (2000-3000 cm^{-1}) of Particle II. (G-I) Enlarged view of the spectra (2000-3000 cm^{-1}) of Particle III. Arrows indicate the band (2600 cm^{-1}) attributed to thiol groups. (J-L) Enlarged view of the spectra (2000-3000 cm^{-1}) of Particle IV.

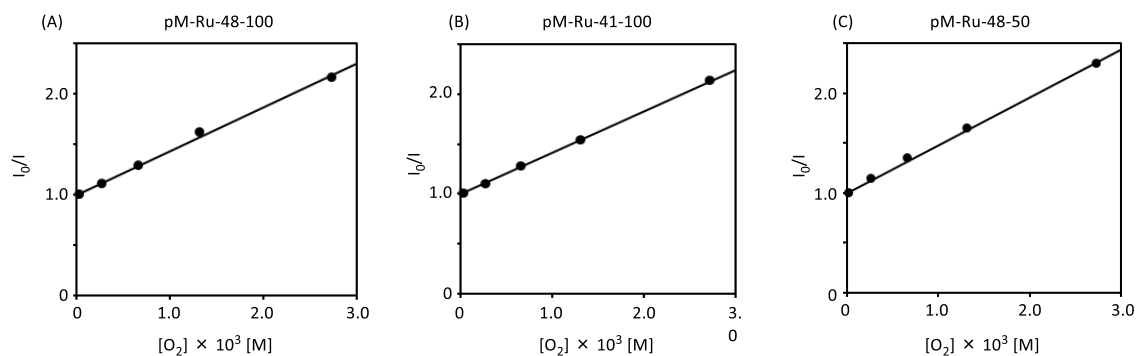


Figure S6. Stern–Volmer plot of the relative phosphorescence intensity (I_0/I) of pM-Rus in the presence of oxygen as a quencher. The relative emission intensities of pM-Ru-48-100 (A), pM-Ru-41-100 (B) and pM-Ru-48-50 (C) were plotted against the oxygen concentration.

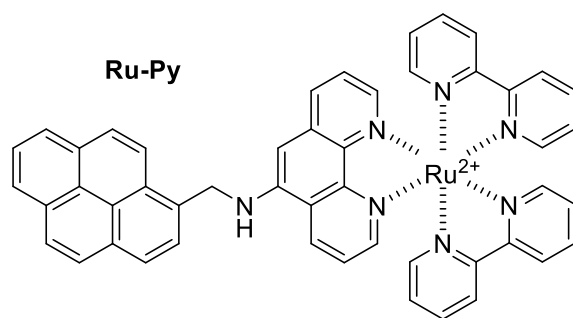


Figure S7. Chemical structure of Ru-Py.

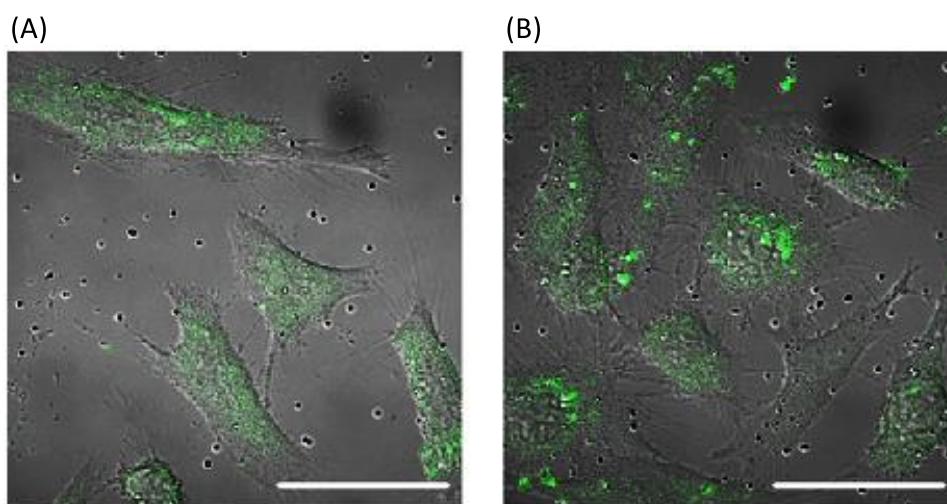


Figure S8. Visualization of singlet oxygen generated in HeLa cells by photoirradiation in the presence of pM-Ru-48-100 (A) and pM-Ru-41-100 (B). Scale bar: 50 μm .